Inorganic Chemistry

pubs.acs.org/IC

Article

Fast Hydrolysis and Strongly Basic Water Adducts Lead to Potent Os(II) Half-Sandwich Anticancer Complexes

Sonia Infante-Tadeo, Vanessa Rodríguez-Fanjul, Cintia C. Vequi-Suplicy, and Ana M. Pizarro*

Cite This: *Inorg. Chem.* 2022, 61, 18970−18978

Read Online

ACCESS | Metrics & More | Article Recommendations | Supporting Information

ABSTRACT: Complexes of the formula [Os(η^6-arene)(*C*,*N*-phenylpyridine)Z] (where Z is chlorido or a tethered oxygen) undergo very fast Os−Z hydrolysis (<5 min), and the high basicity of the coordinated water molecule of the aqua adducts (Os−OH_2; pK_a > 8) very much contrasts with previously reported Os-aqua adducts bearing NN- and NO-chelating ligands (pK_a < 6). The Os−Cl bond is unreactive in pure DMSO, yet the complexes readily form DMSO adducts upon aquation when dimethyl sulfoxide is present. Such a peculiar aqueous behavior is directly related to the negatively charged CN ligand. Potent Os-CN compounds (but not their Os-NN analogues) are particularly reactive; they bind to cysteine in vitro and decrease the activity of thioredoxin reductase (TrxR) in living cancer cells. By revealing some interesting structure−activity relationship on Os-CN vs Os-NN complexes, we start uncovering the molecular rationale for the successful biological applications of osmium(II) half-sandwich compounds.

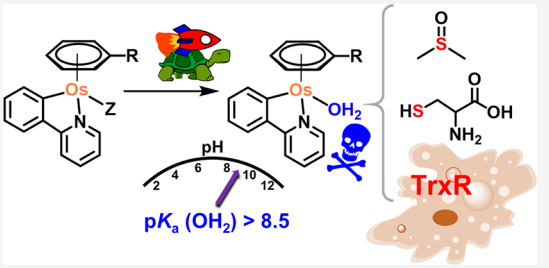

INTRODUCTION

Cisplatin, or cis-diamminedichloridoplatinum(II), is one of the most widely used drugs in cancer chemotherapy. Its mode of action to stop cell replication involves coordinative binding to DNA upon aquation of the Pt−Cl bonds inside the cell, that is, a water molecule replaces each chlorido ligand, and a further substitution reaction results in Pt-guanine coordination.[1]

Initial interest in anticancer osmium half-sandwich complexes of the formula [Os(η^6-arene)(κ^2-XY)Cl]$^+$ that fit into the activation-through-hydrolysis paradigm was sparked by Peacock et al., who successfully activated Os reactivity in water by carefully selecting the XY chelating ligand.[2−4] A relationship was established between the coordinative nature of XY, Os−Cl aquation, and the acidity of the subsequently Os-κ^1-bound water molecule. Complexes with neutral NN ligands hardly hydrolyzed (and were thus unreactive toward substitution reactions and inactive toward cancer cells),[5−7] while anionic OO ligands had the opposite effect, producing fast hydrolyzing complexes.[3,8] Rapid aquation combined with high acidity of Os-bound water triggered the formation of noncytotoxic inert hydroxido-bridged dimers, [Os(η^6-arene)(μ^2-OH)$_3$Os(η^6-arene)]$^+$, concomitant to the XY ligand loss.[2] Os-picolinate complexes (NO-chelating ligands), with faster hydrolysis and pK_a(Os−OH_2) closer to physiological pH, showed moderate in vitro cytotoxicity, approaching that of carboplatin.[2,8]

In a quest to find hydrolyzable, and intracellularly reactive, organo-osmium compounds, we recently reported Os-arenes bearing a pendant alcohol functionality to bypass the inert hydroxido-bridge dimer formation, as the Os-hydroxido (Os−OH) adduct triggers intramolecular rearrangement that culminates in the binding of the pendant alcohol to the metal center (formation of tethered alkoxy complexes), thus ensuring kinetic reactivation of osmium in water.[5]

In the past years, potent hydrolyzable Os-chlorido complexes [Os(η^6-arene)(CN)Cl]$^+$, where CN is an anionic κ^2-*C*,*N*-binding ligand such as a phenylazole (including phenylbenzimidazole) derivative[9−12] or phenylpyridine[12−15] and η^6-arene is benzene or *p*-cymene, have been reported by Ruiz et al. and Keppler et al. Such complexes present IC_{50} values in several cancer cell lines up to one order of magnitude lower than cisplatin. Interestingly, the Os(II)-arene-CN half-sandwich structure is reminiscent of those of Ru(II)-arene-CN,[16−19] Ir(III)-Cp*-CN,[20−22] and Rh(III)-Cp*-CN,[23] and it might seem that when looking for cytotoxic potency of metallodrug candidates, it is the anionic CN ligand that ensures such a goal. Nevertheless, the molecular rationale behind why half-sandwich Os(II) compounds bearing anionic CN-chelates remain some of the most potent organo-osmium compounds to date is elusive, despite being fundamental to understanding how potent organo-osmiums exert their intracellular effect.

Dimethyl sulfoxide is a common solvent used in cell studies to aid dissolution for the testing of lipophilic drugs. In addition, DMSO can be considered a strongly coordinating

Received: September 12, 2022
Published: November 15, 2022

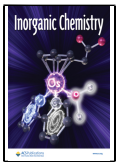

https://doi.org/10.1021/acs.inorgchem.2c03246
Inorg. Chem. 2022, 61, 18970−18978

molecule, and a few interesting studies have demonstrated that it may be a noninnocent vehicle during biological studies as it can mediate metal-based unexpected reactivity.[24,25] Sulfur (and selenium) coordination to transition metals has not been overlooked in the interaction of metallodrugs with the thioredoxin reductase (TrxR) system. TrxR inhibition by metal-based compounds is well-documented and expectedly involves ligand exchange reactions at a labile position in the first coordination sphere of the metal with SeCys and Cys residues at the enzyme active site.[26−30] Recent studies have indicated that the TrxR activity is weakly affected by cytotoxic compounds based on osmium,[31] while it is strongly inhibited by Au-,[32,33] Ru-,[34,35] and Ir-based[22] anticancer candidates.

We present here a series of experiments in water on very potent Os(II)-CN complexes that appear to unveil, at the molecular level, what are the principles for maintaining Os-based chemical reactivity in aqueous media and thus Os-mediated anticancer potency. Our results on the aqueous behavior of complexes of the type $[Os(\eta^6\text{-arene})(C,N\text{-phenylpyridine})Z]^+$ successfully relate their strong in vitro cytotoxicity to the reactivity of the Os−Z bond and the basicity of the Os-coordinated water upon aquation. The persistence of the Os−OH_2 bond in water appears to drive Os-based reactivity, in particular with S-containing molecules, outside and inside the cancer cell.

EXPERIMENTAL SECTION

η^6-Bound arenes containing electron-withdrawing groups such as esters are thermally labile when coordinated to Ru(II), which has been extensively exploited in the preparation of Ru(II) dimers containing mono- and disubstituted arenes for a number of applications.[36−41] However, arene exchange reactions proved ineffective for osmium using $[Os(\eta^6\text{-Et/Me-benzoate})(\mu\text{-Cl})Cl]_2$ as the starting material. The preparation of the complexes described in this work thus required to reduce the arene hemilabile ligands 2-phenylacetic acid and 3-phenylpropanoic acid to the corresponding cyclohexadienes, prior to the reaction with $OsCl_3{\cdot}3H_2O$ to obtain dimers $[Os(\eta^6\text{-}C_6H_5(CH_2)_nCOOH)(\mu\text{-Cl})Cl]_2$, precursors of **1** ($n$ = 1) and **2** (n = 2). For dimers $[Os(\eta^6\text{-}C_6H_5(CH_2)_nCOOEt)(\mu\text{-Cl})Cl]_2$, which are the dimer precursors of **3** (n = 1) and **4** (n = 2), $OsCl_3{\cdot}3H_2O$ was also reacted with the same reduced versions of 2-phenylacetic acid and 3-phenylpropanoic acid, yet in these reactions, esterification of the carboxylic groups was achieved by using ethanol as the solvent, as previously described for similar ester-derivatized ruthenium(II) dimers,[42] in a one-pot microwave-assisted synthesis.[43] The dimer precursor of complex **5**, $[Os(\eta^6\text{-}C_6H_5(CH_2)_3OH)(\mu\text{-Cl})Cl]_2$, was obtained by reacting $OsCl_3{\cdot}3H_2O$ with the reduced version of 3-phenylpropanol, as previously described by us.[5] The detailed syntheses of the organic ligands and the individual dimers are included in the Supporting Information.

Synthesis of Os(II) Complexes 1−5. *$[Os(\eta^6{:}\kappa^1\text{-}C_6H_5CH_2COO)(Phpy)]$ (**1**).* $[Os(\eta^6\text{-}C_6H_5CH_2COOH)(\mu\text{-Cl})Cl]_2$ (22 mg, 0.028 mmol) and sodium acetate (NaOAc; 37 mg, 0.14 mmol) were stirred for 1 h in 3 mL of DCM at 333 K. After that, 2-phenylpyridine (Phpy; 8 μL, 0.056 mmol) was added to the solution, and the mixture was stirred at 333 K for 3 days. The black suspension was filtered over a pad of Celite, the yellow-green solvent was reduced in a rotary evaporator until it was one-fourth of the initial volume, and then, a yellow-green powder precipitated after the addition of Et_2O. The powder was washed with diethyl ether and dried under reduced pressure. Yield: 21 mg, 0.044 mmol, 78%. Yellow-green crystals suitable for X-ray diffraction were obtained of the complex $[Os(\eta^6{:}\kappa^1\text{-}C_6H_5CH_2COO)(Phpy)]{\cdot}1.5CH_2ClCH_2Cl$ (**1**·1.5DCE) by slow evaporation of a layer diffusion of DCE/pentane at 253 K. ^{1}H NMR (400 MHz, $CDCl_3$, δ): 9.07 (d, J = 5.7 Hz, 1H, PhpyH), 8.09 (d, J = 7.5 Hz, 1H, PhpyH), 7.82 (d, J = 8.1 Hz, 1H, PhpyH), 7.74−7.66 (m, 2H, PhpyH), 7.14 (td, J = 7.3, 1.3 Hz, 1H, PhpyH), 7.11−7.01 (m, 2H, PhpyH), 5.85 (d, J = 4.9 Hz, 1H, ArH), 5.79 (d, J = 5.3 Hz, 1H, ArH), 5.49 (d, J = 5.5 Hz, 1H, ArH), 5.06 (d, J = 4.8 Hz, 1H, ArH), 4.97 (t, J = 5.0 Hz, 1H, ArH), 3.57 (d, J = 17.1 Hz, 1H, $ArCH_2$), 3.41 (d, J = 17.1 Hz, 1H, $ArCH_2$). $^{13}C\{^1H\}$ NMR (101 MHz, $CDCl_3$, δ): 192.80 (s, CO), 167.33 (s, PhpyC), 164.27 (s, PhpyC), 154.40 (s, PhpyCH), 144.80 (s, PhpyC), 139.05 (s, PhpyCH), 137.85 (s, PhpyCH), 130.56 (s, PhpyCH), 124.22 (s, PhpyCH), 123.95 (s, PhpyCH), 122.52 (s, PhpyCH), 119.32 (s, PhpyCH), 90.11 (s, ArC), 88.13 (s, ArCH), 84.56 (s, ArCH), 79.68 (s, ArCH), 64.43 (s, ArCH), 56.73 (s, ArCH), 42.23 (s, $ArCH_2$). MS (ESI): m/z calcd for $C_{19}H_{15}NO_2Os$ $[M + H^+]^+$, 482.1; found, 482.2. Elemental analysis (EA): calcd for $C_{19}H_{15}NO_2Os{\cdot}H_2O$ (497.55): C, 45.87; H, 3.44; N, 2.82%. Found: C, 45.53; H, 3.45; N, 2.78%. Melting point (MP): 130−167 °C.

*$[Os(\eta^6{:}\kappa^1\text{-}C_6H_5CH_2CH_2COO)(Phpy)]$ (**2**).* Synthesis as for **1**, using $[Os(\eta^6\text{-}C_6H_5CH_2CH_2COOH)(\mu\text{-Cl})Cl]_2$ (28 mg, 0.034 mmol), NaOAc (45 mg, 0.17 mmol), and Phpy (10.2 μL, 0.07 mmol). Yield: 28 mg, 0.057 mmol, 83%. ^{1}H NMR (400 MHz, DMSO-d_6, δ): 9.30 (d, J = 5.9 Hz, 1H, PhpyH), 8.14−8.08 (m, 2H, PhpyH), 7.92 (s, 1H, PhpyH), 7.84−7.80 (m, 1H, PhpyH), 7.23 (s, 1H, PhpyH), 7.03 (dd, J = 8.6, 3.3 Hz, 2H, PhpyH), 6.08 (t, J = 5.4 Hz, 1H, ArH), 5.89 (d, J = 5.9 Hz, 1H, ArH), 5.76 (t, J = 4.9 Hz, 1H, ArH), 5.62 (d, J = 5.0 Hz, 1H, ArH), 4.91 (t, J = 5.0 Hz, 1H, ArH), 3.57 (s, 2H, ArCH), 3.04−2.92 (m, 1H, CH_2O), 2.41−2.37 (m, 1H, CH_2O). $^{13}C\{^1H\}$ NMR (101 MHz, $CDCl_3$, δ): 177.31 (s, CO), 167.18 (s, PhpyC), 164.86 (s, PhpyC), 154.47 (s, PhpyCH), 145.28 (s, PhpyC), 138.36 (s, PhpyCH), 137.85 (s, PhpyCH), 130.62 (s, PhpyCH), 124.39 (s, PhpyCH), 123.72 (s, PhpyCH), 122.71 (s, PhpyCH), 119.36 (s, PhpyCH), 95.79 (s, ArC), 86.99 (s, ArCH), 82.79 (s, ArCH), 81.11 (s, ArCH), 64.20 (s, ArCH), 58.18 (s, ArCH), 36.75 (s, CH_2CO), 28.84 (s, $ArCH_2$). MS (ESI): m/z calcd for $C_{20}H_{18}NO_2Os$ $[M + H^+]^+$, 496.1; found, 496.3. EA: calcd for $C_{20}H_{17}NO_2Os{\cdot}H_2O$ (511.58): C, 46.96; H, 3.74; N, 2.74%. Found: C, 47.00; H, 3.75; N, 2.6%. MP: 90−120 °C.

*$[Os(\eta^6\text{-}C_6H_5CH_2COOEt)(Phpy)Cl]$ (**3**).* Synthesis as for **1**, using $[Os(\eta^6\text{-}C_6H_5CH_2COOEt)(\mu\text{-Cl})Cl]_2$ (30 mg, 0.035 mmol), NaOAc (7.8 mg, 0.097 mmol), and Phpy (9.6 μL, 0.07 mmol). The yellow-green powder precipitated after the addition of hexane into the solution, and this powder was washed with hexane and dried. Yellow-orange crystals suitable for X-ray diffraction were obtained of the complex $[Os(\eta^6\text{-}C_6H_5CH_2COOEt)(Phpy)Cl]{\cdot}0.5H_2O$ (**3**·0.5H_2O) by slow evaporation of a triple-layer diffusion of DCM/toluene/hexane (2:3:1) at 253 K. Yield: 25 mg, 0.046 mmol, 66%. ^{1}H NMR (400 MHz, $CDCl_3$, δ): 9.13 (d, J = 5.6 Hz, 1H, PhpyH), 8.02 (d, J = 7.4 Hz, 1H, PhpyH), 7.80 (d, J = 8.1 Hz, 1H, PhpyH), 7.72−7.62 (m, 2H, PhpyH), 7.16 (t, J = 6.9 Hz, 1H, PhpyH), 7.10−6.94 (m, 2H, PhpyH), 5.71 (dd, J = 10.4, 5.3 Hz, 2H, ArH), 5.53 (t, J = 5.2 Hz, 1H, ArH), 5.44 (d, J = 5.4 Hz, 1H, ArH), 5.25 (t, J = 5.1 Hz, 1H, ArH), 4.16 (q, J = 7.1 Hz, 2H, OCH_2), 3.32 (d, J = 6.0 Hz, 2H, $ArCH_2$), 1.26 (t, J = 7.1 Hz, 3H, CH_3). $^{13}C\{^1H\}$ NMR (101 MHz, $CDCl_3$, δ): 171.14 (s, CO), 166.85 (s, PhpyC), 165.32 (s, PhpyC), 155.15 (s, PhpyCH), 144.23 (s, PhpyC), 139.11 (s, PhpyCH), 137.22 (s, PhpyCH), 130.76 (s, PhpyCH), 124.28 (s, PhpyCH), 123.10 (s, PhpyCH), 122.51 (s, PhpyCH), 119.15 (s, PhpyCH), 87.60 (s, ArC), 83.43 (s, ArCH), 79.23 (s, ArCH), 77.16 (s, ArCH), 74.64 (s, ArCH), 72.06 (s, ArCH), 61.33 (s, OCH_2), 39.31 (s, $ArCH_2$), 14.30 (s, CH_3). MS (ESI): m/z calcd for $C_{21}H_{20}NO_2Os$ $[M-Cl^-]^+$, 510.11; found, 509.9. EA: calcd for $C_{21}H_{20}ClNO_2Os{\cdot}H_2O$ (562.07): C, 44.88; H, 3.95; N, 2.49%. Found: C, 45.07; H, 3.87; N, 2.45%. MP: 125−149 °C.

*$[Os(\eta^6\text{-}C_6H_5CH_2CH_2COOEt)(Phpy)Cl]$ (**4**).* Synthesis as for **3**, using $[Os(\eta^6\text{-}C_6H_5CH_2CH_2COOEt)(\mu\text{-Cl})Cl]_2$ (30 mg, 0.034 mmol), NaOAc (7.5 mg, 0.094 mmol), and Phpy (9.6 μL, 0.07 mmol). Yield: 32 mg, 0.057 mmol, 84%. Yellow crystals suitable for X-ray diffraction were obtained in a solution of Et_2O at RT. ^{1}H NMR (400 MHz, $CDCl_3$, δ): 9.13 (d, J = 5.6 Hz, 1H, PhpyH), 8.05 (d, J = 7.4 Hz, 1H, PhpyH), 7.81 (d, J = 8.1 Hz, 1H, PhpyH), 7.67 (dd, J = 15.1, 7.5 Hz, 2H, PhpyH), 7.15 (t, J = 7.2 Hz, 1H, PhpyH), 7.03 (dd, J = 11.8, 6.5 Hz, 2H, PhpyH), 5.67 (t, J = 5.2 Hz, 1H, ArH), 5.58 (d, J = 5.3 Hz, 1H, ArH), 5.49 (t, J = 5.2 Hz, 1H, ArH), 5.38 (d, J = 5.3 Hz, 1H, ArH), 5.24 (t, J = 5.0 Hz, 1H, ArH), 4.12 (q, J = 7.1 Hz, 2H,

https://doi.org/10.1021/acs.inorgchem.2c03246
Inorg. Chem. 2022, 61, 18970−18978

OCH_2), 2.73−2.56 (m, 4H, ArCH_2 overlapped with CH_2CO), 1.24 (t, J = 7.1 Hz, 3H, CH_3). $^{13}C\{^1H\}$ NMR (101 MHz, $CDCl_3$, δ): 172.65 (s, CO), 166.88 (s, PhpyC), 165.69 (s, PhpyC), 155.11 (s, PhpyCH), 144.25 (s, PhpyC), 139.15 (s, PhpyCH), 137.12 (s, PhpyCH), 130.67 (s, PhpyCH), 124.25 (s, PhpyCH), 122.97 (s, PhpyCH), 122.46 (s, PhpyCH), 119.10 (s, PhpyCH), 93.77 (s, ArC), 80.95 (s, ArCH), 79.89 (s, ArCH), 77.03 (s, ArCH), 74.36 (s, ArCH), 71.98 (s, ArCH), 60.78 (s, OCH_2), 35.01 (s, CH_2CO), 28.77 (s, $ArCH_2$), 14.36 (s, CH_3). MS (ESI): m/z calcd for $C_{22}H_{22}NO_2Os$ $[M-Cl^-]^+$, 524.13; found, 523.9. EA: calcd for $C_{22}H_{22}ClNO_2Os\cdot 0.5H_2O$ (567.09): C, 46.60; H, 4.09; N, 2.47%. Found: C, 46.57; H, 4.09; N, 2.54%. MP: 158−187 °C.

*[Os(η^6-$C_6H_5(CH_2)_3OH$)(Phpy)Cl] (**5**).* Synthesis as for **1**, using $[Os(\eta^6\text{-}C_6H_5(CH_2)_3OH)(\mu\text{-}Cl)Cl]_2$ (33 mg, 0.04 mmol), NaOAc (9 mg, 0.11 mmol), and Phpy (11 μL, 0.08 mmol). Yield: 31 mg, 0.06 mmol, 75%. ^1H NMR (400 MHz, $CDCl_3$-*d*, δ): 9.13 (d, J = 5.6 Hz, 1H, PhpyH), 8.05 (d, J = 7.4 Hz, 1H, PhpyH), 7.81 (d, J = 8.1 Hz, 1H, PhpyH), 7.67 (dd, J = 17.5, 7.9 Hz, 2H, PhpyH), 7.15 (t, J = 7.3 Hz, 1H, PhpyH), 7.03 (dd, J = 13.7, 6.8 Hz, 2H, PhpyH), 5.69 (t, J = 5.2 Hz, 1H, ArH), 5.56 (d, J = 5.3 Hz, 1H, ArH), 5.49 (t, J = 5.2 Hz, 1H, ArH), 5.34 (d, J = 5.3 Hz, 1H, ArH), 5.19 (t, J = 5.0 Hz, 1H, ArH), 3.68 (t, J = 6.1 Hz, 2H, CH_2OH), 2.62−2.42 (m, 2H, $ArCH_2$), 1.93−1.75 (m, 2H, CH_2). $^{13}C\{^1H\}$c NMR (101 MHz, $CDCl_3$-*d*, δ): 166.91 (s, PhpyC), 165.79 (s, PhpyC), 155.12 (s, PhpyCH), 144.32 (s, PhpyC), 139.19 (s, PhpyCH), 137.08 (s, PhpyCH), 130.62 (s, PhpyCH), 124.22 (s, PhpyCH), 122.92 (s, PhpyCH), 122.44 (s, PhpyCH), 119.06 (s, PhpyCH), 96.82 (s, ArC), 80.39 (d, J = 16.8 Hz, ArCH), 73.26 (s, ArCH), 70.49 (s, ArCH), 62.14 (s, CH_2OH), 32.87 (s, CH_2), 29.57 (s, $ArCH_2$). MS (ESI): m/z calcd for $C_{20}H_{20}NOOs$ $[M-Cl]^+$, 482.1; found, 481.7. EA: calcd for $C_{20}H_{20}ClNOOs\cdot H_2O$ (534.06): C, 44.98; H, 4.15; N, 2.62%. Found: C, 44.80; H, 3.98; N, 2.74%.

Synthesis of metal complexes bearing bipyridine for comparison purposes and details of chemicals and instrumentation, chemical characterization, pH* measurements, X-ray crystallographic analysis, cell culturing techniques, and cell-based assays are included in detail in the Supporting Information.

RESULTS AND DISCUSSION

We present for the first time complexes **1**−**5** (Chart 1) of general formulae $[Os(\eta^6\text{:}\kappa^1\text{-}C_6H_5(CH_2)_nCOO)(Phpy)]$

Chart 1. Structures of Open and Closed Tethered Osmium(II) Arene Compounds 1−5 Included in This Work

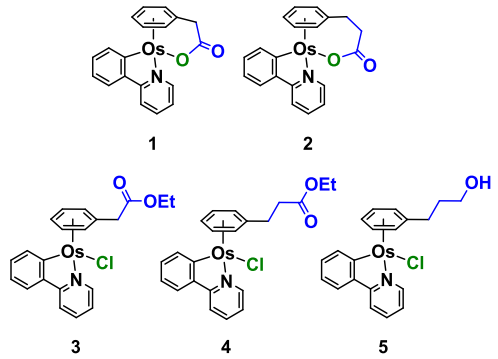

(where Phpy = C,N-phenylpyridine; n = 1, **1**; n = 2, **2**), $[Os(\eta^6\text{-}C_6H_5(CH_2)_nCOOEt)(Phpy)Cl]$ (n = 1, **3**; n = 2, **4**), and $[Os(\eta^6\text{-}C_6H_5(CH_2)_3OH(Phpy)Cl]$ (**5**). Complexes **1** and **2** are tethered complexes, that is, there is no chlorido in the structure and the monodentate position (Z in the general structure $[Os(\eta^6\text{-arene})(Phpy)Z]$) is occupied by the pendant κ^1-O-bound carboxylate (COO^-). The Os−O bond in tether complexes is prone to cleavage in water in a process akin to Os−Cl aquation. Complexes **3** and **4**, containing an ester functionality, cannot form a tether ring, while complex **5** readily affords the tethered structure $[Os(\eta^6\text{:}\kappa^1\text{-}C_6H_5(CH_2)_3O\text{-}(H))(Phpy)]^{0/+}$, whereby the alcohol pendant from the arene is κ^1-O-binding to Os (forming a tether ring in the same fashion as complexes **1** and **2**) in basic aqueous solution (vide infra).

Compounds **1**−**5** were synthesized in good yield (66−84%) by the reaction of the corresponding dimer with deprotonated phenylpyridine, using procedures similar to those reported previously (Chart S1).[10,12,13,19] Experimental details as well as individual characterization are detailed in the Experimental Section and Supporting Information of this manuscript (Figures S1−S14 and Table S1).

Stodt et al. successfully synthesized Ru-arenes bearing a pendant carboxylate, demonstrating that the pendant-arm fragment $\{Ru(\eta^6\text{-}C_6H_5(CH_2)_3COOH)\}$ was suitable for both N-terminal labeling of amino acids and peptides and esterification when the dimer formation was carried out in ethanol.[42] In fact, a number of Ru(II) half-sandwich complexes are reported that bear derivatized arenes for further tagging of proteins,[44] specific protein inhibitors,[45] drugs,[46] or fluorophores.[47] Derivatization of Os(II) arenes is far less exploited,[48,49] perhaps due to the lack of access to arene exchange reactions in Os(II) arene dimers bearing electron-withdrawing groups such as esters.[36] Murray recently reported the formation of $[Os(\eta^6\text{-}3\text{-}(p\text{-tolyl})propanoic\ acid)Cl_2]_2$, following acidic hydrolysis of undesired $[Os(\eta^6\text{-ethyl-}3\text{-}(p\text{-tolyl})propanoate)Cl_2]_2$.[49] Here, we avoided the esterification of the dimer by reacting the corresponding cyclohexadiene with $OsCl_3\cdot H_2O$ in acetone/water (to obtain the precursors of complexes **1** and **2**) and purposely triggered esterification by carrying out the reaction in ethanol (to obtain the precursors of **3** and **4**). However, to the best of our knowledge, **1** and **2** are the first Os-tethered complexes with a chelating hemilabile arene-carboxylate. Likewise, X-ray crystal structures of Os-tethered complexes are scarce.[5,50] Here, we determined the first X-ray examples of Os(II) half-sandwich complexes with a tethered carboxylate (**1**·1.5DCE; Figure 1A) or an ester functionality pendant from the arene (**3**·0.5H_2O and **4**, Figure 1B,C). Full X-ray analysis and detailed crystallographic data (Tables S2 and S3) are included in the Supporting Information.

The in vitro cytotoxic activity of **1**−**5** was investigated in triple negative MDA-MB-231 breast cancer cells. All complexes consistently impaired cell survival at a lower concentration than cisplatin, ranging within 1.9−6.6 μM, while IC_{50}(cisplatin) was 13.7 ± 0.6 μM (Figure 2 and Table S4). The high potency of **5** (2.1 ± 0.4 μM) strikingly contrasts with the moderate potency of analogues $[Os(\eta^6\text{-}C_6H_5(CH_2)_3OH\text{-}(XY)Cl]$, bearing a variety of NN- and NO-chelating ligands.[5] For the latter, the lowest IC_{50} values in MDA-MB-231 cells were 90.6 ± 4.0 and 93.0 ± 4.3 μM, when XY was 4-Me-picolinate or quinolinate, respectively, that is, the most active complexes were over 40-fold less active than complex **5** in this work. The cytotoxicity of **5** was also evaluated in MCF7 and HCT116 cancer cells with comparable results (IC_{50} = 2.8 ± 0.1 and IC_{50} = 5.5 ± 1.5 μM, respectively; Table S4).

Intracellular accumulation of **1**−**5** ([Os] = 10 μM, 8 h drug exposure) was determined in MDA-MB-231 cells by means of ICP-MS. Results were in the range of 61−83 ng Os/10^6 cells for all but **2**, which showed a lower accumulation than the others (29 ng Os/10^6 cells), correlating well with its slightly

https://doi.org/10.1021/acs.inorgchem.2c03246
Inorg. Chem. 2022, 61, 18970−18978

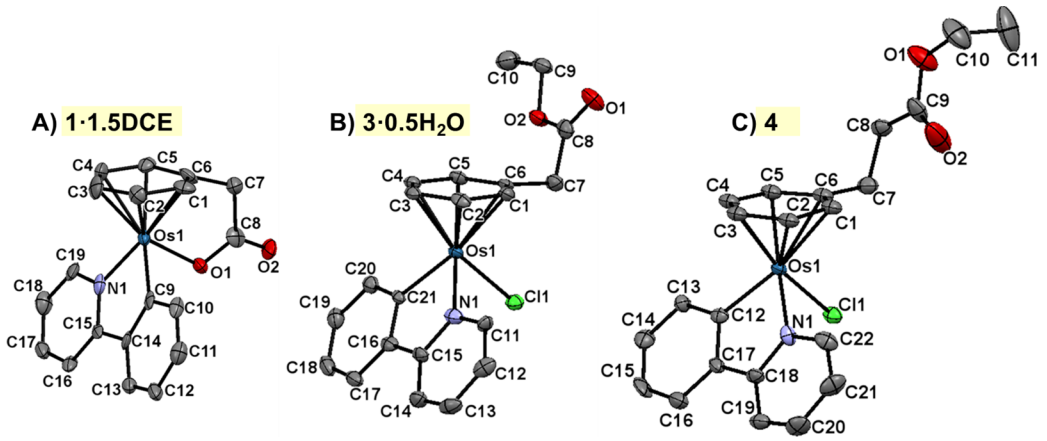

Figure 1. ORTEP diagrams and atom numbering schemes for compounds: (A) **1**·1.5DCE, (B) **3**·0.5H_2O, and (C) **4** (50% probability ellipsoids). The H atoms and the solvent molecules are omitted for clarity.

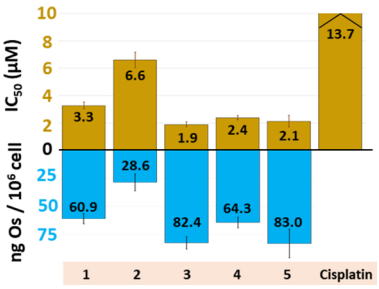

Figure 2. Antiproliferative activity and intracellular accumulation of Os(II) complexes in MDA-MB-231 cells.

lower potency (Figure 2). Accumulation of **5** in MCF7 and HCT116 cells afforded similar results (Table S5).

We aimed at unraveling the molecular basis that relates the strong in vitro cytotoxicity of Os-arenes **1**−**5** with the presence of a phenylpyridine in the structure, for which we explored Os-mediated chemical reactivity. The cleavage of the Os−O(tether) bond in **1** and **2** and the Os−Cl bond in **3**−**5** complexes was monitored by ^{1}H NMR ([Os] = 5 mM) at various time intervals in pure DMSO-d_6, DMSO-d_6/D_2O (5:95), and 300 mM NaCl DMSO-d_6/D_2O (5:95). We expected that, albeit slowly, complexes **1**−**5** interacted with pure DMSO readily forming metal−DMSO adducts.[12,51] However, no significant changes were observed in the first 24 h for **2**−**5** in pure DMSO, while complex **1** was not totally unreactive toward DMSO, as it slowly evolved to form **1DMSO** (22% conversion after 17 h) as determined by ^{1}H NMR (Figure 3A, black dots and diamonds for **1** and **2**, respectively; Figure 3B, black triangles for **5**). The different behavior of **1** at longer times is attributed to the higher tether-ring tension, as the shorter tether arm generates a 5-membered tether ring (see the large C7 offset toward osmium in the X-ray structure of **1**·1.5DCE, Figure 1 and Table S2), ultimately affording an Os−O bond more prone to dissociation.

The lack of solvent coordination in pure DMSO was surprising when contrasted to the readiness to form Os−DMSO adducts when the complexes were dissolved in aqueous solution containing 5% DMSO (that is, an excess of about 140 mol equivalents of DMSO per mol of Os(II) complex). When water was present, **1**−**5** readily converted into **1DMSO**−**5DMSO**. The percentage of disappearance of closed tethered **1** and **2**, and the percentage of newly formed DMSO adducts in chlorido complex **5**, based on ^{1}H NMR peak integration, was plotted against time, fitted to pseudo-first-order kinetics, and their half-life was calculated (Figure 3A,B, insets). The ^{1}H NMR spectra of **1** and **2** showed three species coexisting in solution over time: the initial tethers (**1** and **2**), the aqua adducts (**1A** and **2A**), and the DMSO adducts (**1DMSO** and **2DMSO**; Figure S15). For open chlorido complexes **3**−**5**, two species are observed in solution, the aqua and DMSO adducts, as interconversion occurred and a new sharp singlet appears over time at ca. 2.2 ppm in the ^{1}H NMR spectra, attributable to the coordinated DMSO ligand (Figure S16).[52−54]

Both the Os−O(tether) bond (in **1** and **2**) and the Os−Cl bond (in **3**−**5**) undergo similar fate in DMSO:D_2O when NaCl (ca. 300 mM) is present, as complexes **1**−**5** rapidly evolve to DMSO adducts **1DMSO**−**5DMSO** (Figure 3A,B, orange lines) even with excess chloride ions in solution. Likewise, incorporation of DMSO into the first coordination sphere of Os prevailed even in the presence of cell culture media components, such as inorganic salts, amino acids, and vitamins (Table S6), even containing fetal bovine serum (FBS), for over 24 h by ^{1}H NMR. An interaction with media components was not observed as the DMSO adduct was still favored in 5% DMSO-d_6/D_2O solutions (Figure S17).

Importantly, when analogous experiments were run in 5% DMF-d_7/D_2O, the aqua adduct was the major species (Figure S18). This encouraged the use of DMF, instead of DMSO, as the vehicle to help dissolve our complexes in aqueous media during the cell studies.

Our results indicate that the aqua adduct acts as an intermediate in the DMSO adduct formation (Figure 3C). Assignment of the rapidly forming aqua adduct was supported by titration experiments in DMF/water solutions (vide infra). This rapid aquation (<5 min) only parallels with that of complexes [Os(η^6-*p*-cymene)(quinol)Cl], reported by Sadler,[2] and [Os(η^6-$C_6H_5(CH_2)_3OH$)(quinol)Cl], by us.[5] Regarding the water-mediated interaction with DMSO, a similar observation has been reported before by Keppler et al., who stated that complexes of the formula [Ru(η^6-*p*-cym)(Phtz)Cl] (Phtz = phenyltriazole derivatives) rapidly evolve to their DMSO counterparts only in the presence of water.[11]

In an attempt to better understand the biological relevance of the Os(II)-DMSO adduct formation, cell viability data were also obtained using DMSO to aid dissolution of the Os(II) complexes. The experiments were run in two different

https://doi.org/10.1021/acs.inorgchem.2c03246
Inorg. Chem. 2022, 61, 18970−18978

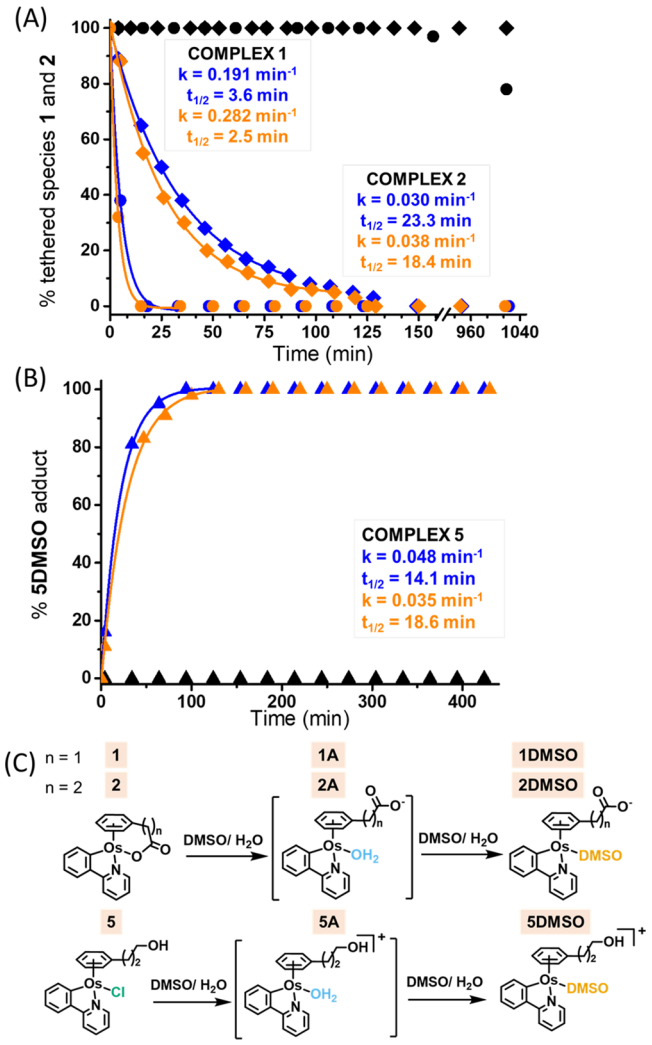

Figure 3. Percentage of (A) tethered Os complexes **1** (dots) and **2** (diamonds) and (B) Os−DMSO adduct formation (**5DMSO**; triangles) over time, as determined by ^{1}H NMR. For (A) and (B), the solutions are as follows: black, pure DMSO; blue, 5% DMSO-d_6 and 95% D_2O; orange, 5% DMSO-d_6 and 95% D_2O, containing 300 mM NaCl. Kinetic constants (k) and half-life ($t_{1/2}$) for the disappearance of tethered complexes **1** and **2** (A) and formation of **5DMSO** (B) are shown in the same color coding. (C) Scheme of speciation into the aqua adduct to readily afford the DMSO adduct. In order to assign formal charges to the organo-osmium compounds that bear ligands prone to acid/base equilibria (containing COO(H) and OH(H) groups), we assume a pH of ca. 7.

conditions: (i) using freshly prepared DMSO/media solutions and (ii) allowing the complexes to stand in the mixture for 24 h at 37 °C prior to addition of the Os(II)-containing solutions to the cells. While the former produced similar data to those using DMF to aid compound dissolution, the latter indicated that DMSO-aged Os(II) solutions failed to impair cell death (reduction in cell viability was not observed at osmium concentrations up to 200 μM; Table S7), further corroborating that the aqua adduct Os-(arene)(C,N)(OH_2) is the active species that ultimately results in cell damage.

Intrigued by the high in vitro cytotoxic potency of rapidly hydrolyzing complexes **1**−**5** and failing to observe inert hydroxido dimeric species in solution, we were prompted to better understand the behavior of the Os−OH_2 aqua adduct. The acid−base equilibrium constant (pK_a) of species **1A**−**5A** [Os(η^6-C_6H_5(R))(Phpy)(**OH_2/OH**)] was determined by means of ^{1}H NMR. Dissolution of neutral and highly hydrophobic **1**−**5** in water required a cosolvent. As for biological studies, DMSO was disfavored to avoid DMSO adduct formation, so noncoordinative DMF was used instead (5% DMF-d_7/D_2O). The Os−Z bond in **1**−**5** hydrolyzed affording aqua adducts **1A**−**5A**. The pK_a values assignable to coordinated water in **1A**−**5A** (pK_{a1}) ranged from 8.73 to 9.38 (Figure 4, blue lines, Table 1, and Figure S19). To the best of

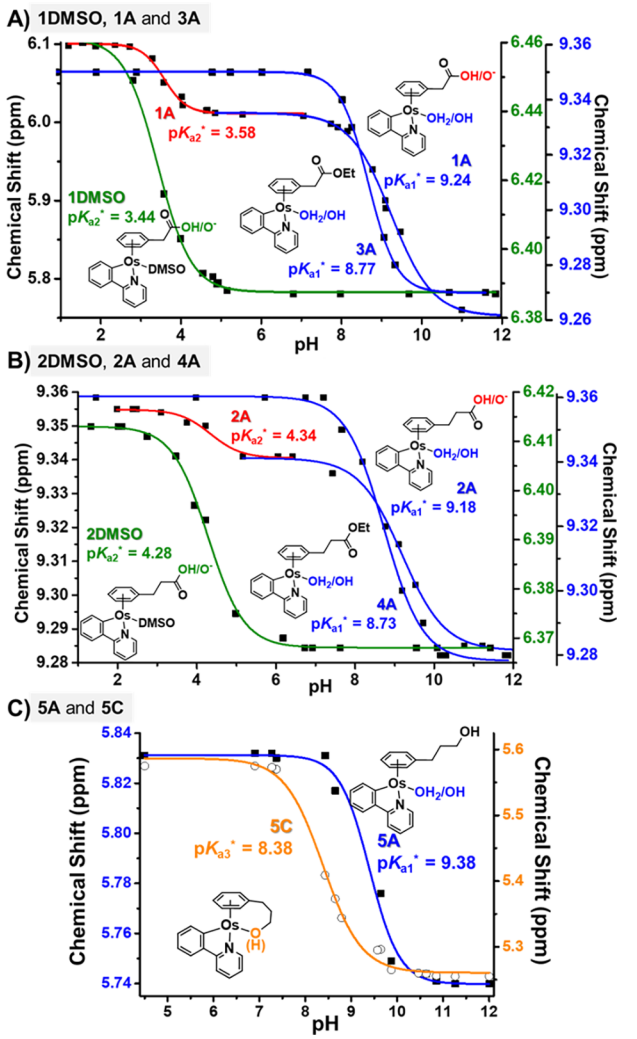

Figure 4. Dependence on pH* (pH in D_2O solutions) of the ^{1}H NMR chemical shifts of osmium complexes. Plots of the chemical shift against pH are fitted to the Henderson−Hasselbalch equation, which afforded the pK_a* values in DMF-d_7/D_2O or DMSO-d_6/D_2O solutions for (A) **1DMSO**, **1A**, and **3A**, (B) **2DMSO**, **2A**, and **4A**, and (C) **5A** and **5C**.

our knowledge, these are the first pK_a(Os−OH_2) reported for Os(II) (and even Ru(II)) half-sandwich complexes containing CN-chelates. Interestingly, they lie in the range of (highly potent) Ir(III)-Cp* complexes also bearing phenylpyridine derivatives (pK_as ranging within 8.3−8.9)[20] and are the most basic pK_as reported to date for Os(II) arenes, with the exception of an Os(η^6-*p*-cym) complex bearing an anionic NN-chelate (deprotonated pyridinylindol).[51] The high basicity of the coordinated water can be attributed to the strong σ-donor CN ligand, which by having a formal negative charge increases

https://doi.org/10.1021/acs.inorgchem.2c03246
Inorg. Chem. 2022, 61, 18970−18978

Table 1. pK_a Values of the Aqua Ligand (pK_{a1}), the Pendant Carboxylic Group (pK_{a2}), and the Tethered Alcohol/Alkoxy Group (pK_{a3}) Corrected from pK_a* by Applying the Equation pH = 0.929 × pH* + 0.42, Suggested by Krężel and Bal[58]

	pK_{a1}	pK_{a2}	pK_{a3}
$[Os(\eta^6\text{-}C_6H_5CH_2COO(H))(Phpy)(OH(H))]^{+/0/-}$ (**1A**)	9.00	3.75	
$[Os(\eta^6\text{-}C_6H_5CH_2COO(H))(Phpy)(DMSO)]^{+/0}$ (**1DMSO**)		3.62	
$[Os(\eta^6\text{-}C_6H_5(CH_2)_2COO(H))(Phpy)(OH(H))]^{+/0/-}$ (**2A**)	8.95	4.45	
$[Os(\eta^6\text{-}C_6H_5(CH_2)_2COO(H))(Phpy)(DMSO)]^{+/0}$ (**2DMSO**)		4.40	
$[Os(\eta^6\text{-}C_6H_5CH_2COOEt)(Phpy)(OH(H))]^{+/0}$ (**3A**)	8.57		
$[Os(\eta^6\text{-}C_6H_5(CH_2)_2COOEt)(Phpy)(OH(H))]^{+/0}$ (**4A**)	8.53		
$[Os(\eta^6\text{-}C_6H_5(CH_2)_3OH)(Phpy)(OH(H))]^{+/0}$ (**5A**)	9.13		
$[Os(\eta^6{:}\kappa^1\text{-}C_6H_5(CH_2)_3O(H))(Phpy)]^{+/0}$ (**5C**)			8.21

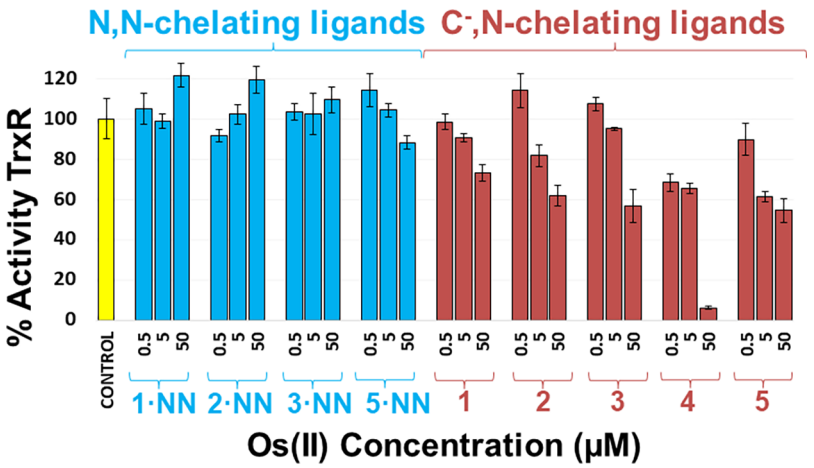

Figure 5. Percentage of the TrxR activity upon exposure of MDA-MB-231 cells to Os(II) complexes, where the blue bars represent Os-NN-bipyridine and red bars represent complexes **1**−**5** (bearing CN-phenylpyridine) described in this work.

electron density on the metal center. Conversely to the high pK_a values of **1A**−**5A** (>8) are those of recently reported aqua adducts $[Os(\eta^6\text{-}C_6H_5(CH_2)_3OH)(NN/NO\text{-chelate})(OH_2)]$, which are <6 for Os-NN and ≤7 for Os-NO complexes.[5] We used DFT calculations on analogues $[Os(\eta^6\text{-}C_6H_6)(Phpy)\text{-}OH_2]^+$ and $[Os(\eta^6\text{-}C_6H_6)(bipy)OH_2]^{2+}$ to assess the electronic distribution in both model complexes. For the Os-NN analogue, osmium donates 0.23 electrons to the three surrounding building blocks (all three ligands, including the bipy). Interestingly, for the Os-CN analogue, the Os center receives 0.08 electrons from its ligands, indicating that the osmium center is significantly more basic (Tables S8 and S9). These results on distinct electronic fluxes of the first coordination sphere of NN versus CN coordination of Os(II) half-sandwich complexes agree with the observations of Needham et al.[55]

We determined the pK_a of the carboxylic acid groups (pK_{a2}) in aqua adducts **1A** and **2A** and also in DMSO adducts **1DMSO** and **2DMSO** (Figure 4 and Table 1). Chart S2 summarizes the speciation in aqueous solution of complexes **1**−**5** both in DMF-d_7/D_2O and in DMSO-d_6/D_2O. Titrations in DMSO-d_6/D_2O helped us to unambiguously corroborate Os−DMSO adduct formation, as none of the titrations in 5% DMSO-d_6/D_2O yielded pK_a data corresponding to the $OH_2 \leftrightarrows$ OH equilibria (pK_{a1}), that is, the species in solution were indeed **1DMSO**−**5DMSO** (Figure 4, Figure S20, and Table 1). Data of pK_{a2} demonstrated the acidity shift (ca. 0.4−0.8 units) of the pendant −COOH group upon metal-arene coordination.[56] Finally, the closed tethered complex $[Os(\eta^6{:}\kappa^1\text{-}C_6H_5(CH_2)_3OH)(Phpy)]$, **5C**, shows a protonation/deprotonation step for the alcohol/alkoxy group (Figure 4C orange) in agreement with our recent results on pH-dependent aqueous speciation of tethered Os(II) arenes bearing phenylpropanol. In such a study, the pK_a of compounds $[Os(\eta^6{:}\kappa^1\text{-}C_6H_5(CH_2)_3\mathbf{OH/O})(NN/NO)]$ ranged within 4.35−5.65.[5] The pK_a value reported here for **5C** (pK_{a3}), 8.38, is extraordinarily high, further supporting the strong effect by the CN-phenylpyridine ligand on the Os center and consequently on the rest of the ligands in the first coordination sphere of the metal. Curiously, formation of **5C** at a basic pH occurred even in the presence of DMSO; in other words, osmium shielding by the tether arm occurs even in competition with strongly coordinating DMSO (Figure S21).

The rapid hydrolysis (activation) of these complexes, the basicity of the water molecule (maintaining the organo-osmium in its activated form) together with the readiness of the complexes to interact with DMSO on aquation, prompted us to probe the reactivity of the complexes against sulfur-containing biomolecules. For this experiment, we compared Os-CN complexes **1**−**5** with their Os-NN counterparts (bearing bipyridine instead of phenylpyridine), as the Os−Cl bond of the latter hardly hydrolyzes and presents a relatively acidic coordinated water molecule (pK_{a1} < 6) upon aquation.[5,6] While the interaction with cysteine (Cys) was easily followed over time for complex **5** by ^{1}H NMR, the analogue **5·NN** $[Os(\eta^6\text{-}C_6H_5(CH_2)_3OH)(bipy)Cl]^+$ did not interact with the S-containing amino acid over 24 h (Figure S22). This observation corroborates the higher chemical reactivity of Os-CN vs Os-NN complexes, and urged us to explore such Os-mediated reactivity inside the cell. To test our hypothesis, we explored the intracellular activity of thioredoxin reductase (TrxR) in MDA-MB-231 cells upon exposure to the

https://doi.org/10.1021/acs.inorgchem.2c03246
Inorg. Chem. 2022, 61, 18970−18978

osmium compounds. TrxR is not only highly relevant in ROS homeostasis (in particular in cancer metabolism) but also, and crucial to our purpose, is rich in cysteine (and SeCys) residues,[57] which might be good nucleophiles in substitution reactions at the Os−OH_2 labile position. We thus compared the effect on the enzymatic activity of TrxR in MDA-MB-231 cells of **1**−**5** with four of their Os-NN analogues. While **1**−**5** decreased the activity of TrxR by ca. 60% (50 μM, 6 h of drug exposure), osmium complexes bearing NN-chelates did not decrease the TrxR activity (Figure 5). This is, to the best of our knowledge, the first study of Os-mediated TrxR inhibition in living cancer cells.

CONCLUSIONS

We report for the first time complexes **1**−**5** of the general formulae [Os(η^6:κ^1-$C_6H_5(CH_2)_nCOO$)(Phpy)] (where Phpy = *C*,*N*-phenylpyridine; n = 1, **1**; n = 2, **2**), [Os(η^6-$C_6H_5(CH_2)_nCOOEt$)(Phpy)Cl] (n = 1, **3**; n = 2, **4**), and [Os(η^6-$C_6H_5(CH_2)_3OH$(Phpy)Cl] (**5**). Complexes **1** and **2** are tethered complexes, that is, the *Z* position in [Os(η^6-arene)(Phpy)Z] is occupied by the pendant κ^1-O-bound carboxylate (COO^-). We have recounted the impact of the phenylpyridine CN coordination on osmium chemical reactivity at the Os−Z bond, from the lack of reactivity in pure DMSO to the readiness to interact with the sulfur-containing molecule upon activation through hydrolysis. Aquation is extraordinarily fast (<5 min), and the coordinated water molecule is extraordinarily basic (pK_a > 8). The Os-mediated reactivity is proven inside cells as per inhibition of TrxR, while osmium does not impact the in-cell TrxR activity when phenylpyridine is replaced by neutral bipyridine. We believe that these are the fundamental basis to design organo-osmium complexes whose intracellular chemical reactivity is understood, thus enabling the development of valid Os-based tools in cancer research.

ASSOCIATED CONTENT

Supporting Information

The Supporting Information is available free of charge at https://pubs.acs.org/doi/10.1021/acs.inorgchem.2c03246.

Experimental details and synthetic procedures for the synthesis of ligands, intermediates, and additional metal complexes for comparison purposes (**1·NN**−**3·NN** and **5·NN**); crystallographic data for **1**·1.5DCE, **3**·0.5H_2O, **4**, **1·NN**·PF_6·MeOH, and **2·NN**·PF_6·MeOH; supporting figures, charts, and tables (PDF)

Accession Codes

CCDC 1860335, 2093402, 2093782, 2093784, and 2093787 contain the supplementary crystallographic data for this paper. These data can be obtained free of charge via www.ccdc.cam.ac.uk/data_request/cif, or by emailing data_request@ccdc.cam.ac.uk, or by contacting The Cambridge Crystallographic Data Centre, 12 Union Road, Cambridge CB2 1EZ, UK; fax: +44 1223 336033.

CCDC 2093782, 2093784, and 2093787 contain the supplementary crystallographic data for tether compound **1**·1.5DCE and open tether compounds **3**·0.5H_2O and **4**, respectively. Complexes **1·NN**·PF_6·MeOH and **2·NN**·PF_6·MeOH have CCDC identifiers 1860335 and 2093402, respectively.

AUTHOR INFORMATION

Corresponding Author

Ana M. Pizarro − *IMDEA Nanociencia, Ciudad Universitaria de Cantoblanco, Madrid 28049, Spain; Unidad Asociada de Nanobiotecnología CNB-CSIC-IMDEA, 28049 Madrid, Spain;* orcid.org/0000-0003-3037-9835; Email: ana.pizarro@imdea.org

Authors

Sonia Infante-Tadeo − *IMDEA Nanociencia, Ciudad Universitaria de Cantoblanco, Madrid 28049, Spain;* Present Address: Department of Cell and Tissue Biology, University of California San Francisco, San Francisco, California 94122, United States; orcid.org/0000-0001-9476-886X

Vanessa Rodríguez-Fanjul − *IMDEA Nanociencia, Ciudad Universitaria de Cantoblanco, Madrid 28049, Spain;* orcid.org/0000-0002-3386-5874

Cintia C. Vequi-Suplicy − *IMDEA Nanociencia, Ciudad Universitaria de Cantoblanco, Madrid 28049, Spain;* orcid.org/0000-0003-1980-5039

Complete contact information is available at: https://pubs.acs.org/10.1021/acs.inorgchem.2c03246

Author Contributions

A.M.P. conceived and designed the study. S.I.-T. developed the synthetic methodology, synthesized the complexes, and carried out the aqueous studies. S.I.-T. and V.R.-F. carried out the experiments in cells and analyzed the data. C.C.V.-S. carried out the theoretical calculations. S.I.-T., V.R.-F., C.C.V.-S., and A.M.P. discussed the findings and contributed toward writing the manuscript. All authors have given approval to the final version of the manuscript.

Notes

The authors declare no competing financial interest.

ACKNOWLEDGMENTS

We thank Dr. J. Perles and Dr. M. Ramírez (Universidad Autónoma de Madrid) for the collection of X-ray data and Dr. Z. Pardo (IMDEA Nanociencia) for assistance with NMR experiments. We acknowledge funding from the EC (FP7-PEOPLE-2013-CIG, no. 631396), from the Spanish MINECO (RYC-2012-11231, SEV-2016-0686, CTQ2017-84932-P, and PID2020-117766GB-I00), and the Comunidad Autónoma de Madrid (Scholarship PEJD-2016/IND-2608).

REFERENCES

(1) Wang, D.; Lippard, S. J. Cellular processing of platinum anticancer drugs. *Nat. Rev. Drug Discovery* **2005**, *4*, 307−320.

(2) Peacock, A. F. A.; Parsons, S.; Sadler, P. J. Tuning the hydrolytic aqueous chemistry of osmium arene complexes with N,O-chelating ligands to achieve cancer cell cytotoxicity. *J. Am. Chem. Soc.* **2007**, *129*, 3348−3357.

(3) Peacock, A. F. A.; Habtemariam, A.; Fernández, R.; Walland, V.; Fabbiani, F. P. A.; Parsons, S.; Aird, R. E.; Jodrell, D. I.; Sadler, P. J. Tuning the reactivity of osmium(II) and ruthenium(II) arene complexes under physiological conditions. *J. Am. Chem. Soc.* **2006**, *128*, 1739−1748.

(4) Fu, Y.; Habtemariam, A.; Pizarro, A. M.; van Rijt, S. H.; Healey, D. J.; Cooper, P. A.; Shnyder, S. D.; Clarkson, G. J.; Sadler, P. J. Organometallic osmium arene complexes with potent cancer cell cytotoxicity. *J. Med. Chem.* **2010**, *53*, 8192−8196.

(5) Infante-Tadeo, S.; Rodríguez-Fanjul, V.; Habtemariam, A.; Pizarro, A. M. Osmium(II) Tethered Half-Sandwich Complexes: pH-

dependent Aqueous Speciation and Transfer Hydrogenation in Cells. *Chem. Sci.* **2021**, *12*, 9287−9297.
(6) Peacock, A. F. A.; Habtemariam, A.; Moggach, S. A.; Prescimone, A.; Parsons, S.; Sadler, P. J. Chloro half-sandwich osmium(II) complexes: Influence of chelated N,N-ligands on hydrolysis, guanine binding, and cytotoxicity. *Inorg. Chem.* **2007**, *46*, 4049−4059.
(7) Meier-Menches, S. M.; Gerner, C.; Berger, W.; Hartinger, C. G.; Keppler, B. K. Structure-activity relationships for ruthenium and osmium anticancer agents - towards clinical development. *Chem. Soc. Rev.* **2018**, *47*, 909−928.
(8) van Rijt, S. H.; Peacock, A. F. A.; Johnstone, R. D. L.; Parsons, S.; Sadler, P. J. Organometallic osmium(II) arene anticancer complexes containing picolinate derivatives. *Inorg. Chem.* **2009**, *48*, 1753−1762.
(9) Yellol, J.; Pérez, S. A.; Buceta, A.; Yellol, G.; Donaire, A.; Szumlas, P.; Bednarski, P. J.; Makhloufi, G.; Janiak, C.; Espinosa, A.; Ruiz, J. Novel C,N-Cyclometalated Benzimidazole Ruthenium(II) and Iridium(III) Complexes as Antitumor and Antiangiogenic Agents: A Structure-Activity Relationship Study. *J. Med. Chem.* **2015**, *58*, 7310−7327.
(10) Ortega, E.; Yellol, J. G.; Rothemund, M.; Ballester, F. J.; Rodríguez, V.; Yellol, G.; Janiak, C.; Schobert, R.; Ruiz, J. A new C,N-cyclometalated osmium(II) arene anticancer scaffold with a handle for functionalization and antioxidative properties. *Chem. Commun.* **2018**, *54*, 11120−11123.
(11) Riedl, C. A.; Flocke, L. S.; Hejl, M.; Roller, A.; Klose, M. H. M.; Jakupec, M. A.; Kandioller, W.; Keppler, B. K. Introducing the 4-Phenyl-1,2,3-Triazole Moiety as a Versatile Scaffold for the Development of Cytotoxic Ruthenium(II) and Osmium(II) Arene Cyclometalates. *Inorg. Chem.* **2017**, *56*, 528−541.
(12) Boff, B.; Gaiddon, C.; Pfeffer, M. Cancer cell cytotoxicity of cyclometalated compounds obtained with osmium(II) complexes. *Inorg. Chem.* **2013**, *52*, 2705−2715.
(13) Cerón-Camacho, R.; Morales-Morales, D.; Hernandez, S.; Le Lagadec, R.; Ryabov, A. D. Easy Access to Bio-Inspired Osmium(II) Complexes through Electrophilic Intramolecular C(sp^2)-H Bond Cyclometalation. *Inorg. Chem.* **2008**, *47*, 4988−4995.
(14) Ryabov, A. D.; Soukharev, V. S.; Alexandrova, L.; Le Lagadec, R.; Pfeffer, M. Low-Potential Cyclometalated Osmium(II) Mediators of Glucose Oxidase. *Inorg. Chem.* **2003**, *42*, 6598−6600.
(15) Ortega, E.; Ballester, F.-J.; Hernández-García, A.; Hernández-García, S.; Guerrero-Rubio, M. A.; Bautista, D.; Santana, M. D.; Gandía-Herrero, F.; Ruiz, J. Novel organo-osmium(II) proteosynthesis inhibitors active against human ovarian cancer cells reduces gonad tumor growth in Caenorhabditis elegans. *Inorg. Chem. Front.* **2020**, *8*, 141−155.
(16) Ruiz, J.; Rodríguez, V.; Cutillas, N.; Espinosa, A.; Hannon, M. J. A potent ruthenium(II) antitumor complex bearing a lipophilic levonorgestrel group. *Inorg. Chem.* **2011**, *50*, 9164−9171.
(17) Belsa, L.; López, C.; González, A.; Font-Bardía, M.; Calvet, T.; Calvis, C.; Messeguer, R. Neutral and Ionic Cycloruthenated 2-Phenylindoles as Cytotoxic Agents. *Organometallics* **2013**, *32*, 7264−7267.
(18) Martínez-Alonso, M.; Busto, N.; Jalón, F. A.; Manzano, B. R.; Leal, J. M.; Rodríguez, A. M.; García, B.; Espino, G. Derivation of structure-activity relationships from the anticancer properties of ruthenium(II) arene complexes with 2-aryldiazole ligands. *Inorg. Chem.* **2014**, *53*, 11274−11288.
(19) Ballester, F. J.; Ortega, E.; Porto, V.; Kostrhunova, H.; Davila-Ferreira, N.; Bautista, D.; Brabec, V.; Domínguez, F.; Santana, M. D.; Ruiz, J. New half-sandwich ruthenium(II) complexes as proteosynthesis inhibitors in cancer cells. *Chem. Commun.* **2019**, *55*, 1140−1143.
(20) Liu, Z.; Habtemariam, A.; Pizarro, A. M.; Clarkson, G. J.; Sadler, P. J. Organometallic Iridium(III) Cyclopentadienyl Anticancer Complexes Containing C N-Chelating Ligands. *Organometallics* **2011**, *30*, 4702−4710.
(21) Liu, Z.; Romero-Canelón, I.; Qamar, B.; Hearn, J. M.; Habtemariam, A.; Barry, N. P. E.; Pizarro, A. M.; Clarkson, G. J.; Sadler, P. J. The potent oxidant anticancer activity of organoiridium catalysts. *Angew. Chem., Int. Ed.* **2014**, *53*, 3941−3946.
(22) Carrasco, A. C.; Rodríguez-Fanjul, V.; Habtemariam, A.; Pizarro, A. M. Structurally strained half-sandwich iridium(III) complexes as highly potent anticancer agents. *J. Med. Chem.* **2020**, *63*, 4005−4021.
(23) Zhang, W. Y.; Bridgewater, H. E.; Banerjee, S.; Soldevila-Barreda, J. J.; Clarkson, G. J.; Shi, H.; Imberti, C.; Sadler, P. J. Ligand-Controlled Reactivity and Cytotoxicity of Cyclometalated Rhodium(III) Complexes. *Eur. J. Inorg. Chem.* **2020**, *2020*, 1052−1060.
(24) Rafols, L.; Josa, D.; Aguilà, D.; Barrios, L. A.; Roubeau, O.; Cirera, J.; Soto-Cerrato, V.; Pérez-Tomás, R.; Martínez, M.; Grabulosa, A.; Gamez, P. Piano-Stool Ruthenium(II) Complexes with Delayed Cytotoxic Activity: Origin of the Lag Time. *Inorg. Chem.* **2021**, *60*, 7974−7990.
(25) Patra, M.; Joshi, T.; Pierroz, V.; Ingram, K.; Kaiser, M.; Ferrari, S.; Spingler, B.; Keiser, J.; Gasser, G. DMSO-Mediated Ligand Dissociation: Renaissance for Biological Activity of N-Heterocyclic-[Ru(η^6-arene)Cl_2] Drug Candidates. *Chem. − Eur. J.* **2013**, *19*, 14768−14772.
(26) Rubbiani, R.; Kitanovic, I.; Alborzinia, H.; Can, S.; Kitanovic, A.; Onambele, L. A.; Stefanopoulou, M.; Geldmacher, Y.; Sheldrick, W. S.; Wolber, G.; Prokop, A.; Wölfl, S.; Ott, I. Benzimidazol-2-ylidene Gold(I) Complexes Are Thioredoxin Reductase Inhibitors with Multiple Antitumor Properties. *J. Med. Chem.* **2010**, *53*, 8608−8618.
(27) Ott, I.; Qian, X.; Xu, Y.; Vlecken, D. H. W.; Marques, I. J.; Kubutat, D.; Will, J.; Sheldrick, W. S.; Jesse, P.; Prokop, A.; Bagowski, C. P. A Gold(I) Phosphine Complex Containing a Naphthalimide Ligand Functions as a TrxR Inhibiting Antiproliferative Agent and Angiogenesis Inhibitor. *J. Med. Chem.* **2009**, *52*, 763−770.
(28) Meyer, A.; Bagowski, C. P.; Kokoschka, M.; Stefanopoulou, M.; Alborzinia, H.; Can, S.; Vlecken, D. H.; Sheldrick, W. S.; Wölfl, S.; Ott, I. On the Biological Properties of Alkynyl Phosphine Gold(I) Complexes. *Angew. Chem., Int. Ed.* **2012**, *51*, 8895−8899.
(29) Bindoli, A.; Rigobello, M. P.; Scutari, G.; Gabbiani, C.; Casini, A.; Messori, L. Thioredoxin reductase: A target for gold compounds acting as potential anticancer drugs. *Coord. Chem. Rev.* **2009**, *253*, 1692−1707.
(30) Oehninger, L.; Stefanopoulou, M.; Alborzinia, H.; Schur, J.; Ludewig, S.; Namikawa, K.; Muñoz-Castro, A.; Köster, R. W.; Baumann, K.; Wölfl, S.; Sheldrick, W. S.; Ott, I. Evaluation of arene ruthenium(II) N-heterocyclic carbene complexes as organometallics interacting with thiol and selenol containing biomolecules. *Dalton Trans.* **2013**, *42*, 1657−1666.
(31) Lam, N. Y. S.; Truong, D.; Burmeister, H.; Babak, M. V.; Holtkamp, H. U.; Movassaghi, S.; Ayine-Tora, D. M.; Zafar, A.; Kubanik, M.; Oehninger, L.; Söhnel, T.; Reynisson, J.; Jamieson, S. M. F.; Gaiddon, C.; Ott, I.; Hartinger, C. G. From Catalysis to Cancer: Toward Structure-Activity Relationships for Benzimidazol-2-ylidene-Derived N-Heterocyclic-Carbene Complexes as Anticancer Agents. *Inorg. Chem.* **2018**, *57*, 14427−14434.
(32) Rodríguez-Fanjul, V.; López-Torres, E.; Mendiola, M. A.; Pizarro, A. M. Gold(III) bis(thiosemicarbazonate) compounds in breast cancer cells: Cytotoxicity and thioredoxin reductase targeting. *Eur. J. Med. Chem.* **2018**, *148*, 372−383.
(33) Meier-Menches, S. M.; Aikman, B.; Döllerer, D.; Klooster, W. T.; Coles, S. J.; Santi, N.; Luk, L.; Casini, A.; Bonsignore, R. Comparative biological evaluation and G-quadruplex interaction studies of two new families of organometallic gold(I) complexes featuring N-heterocyclic carbene and alkynyl ligands. *J. Inorg. Biochem.* **2020**, *202*, No. 110844.
(34) Kladnik, J.; Kljun, J.; Burmeister, H.; Ott, I.; Romero-Canelón, I.; Turel, I. Towards Identification of Essential Structural Elements of Organoruthenium(II)-Pyrithionato Complexes for Anticancer Activity. *Chem. − Eur. J.* **2019**, *25*, 14169−14182.

https://doi.org/10.1021/acs.inorgchem.2c03246
Inorg. Chem. 2022, 61, 18970−18978

(35) Pettinari, R.; Marchetti, F.; Di Nicola, C.; Pettinari, C. Half-Sandwich Metal Complexes with β-Diketone-Like Ligands and Their Anticancer Activity. *Eur. J. Inorg. Chem.* **2018**, *2018*, 3521−3536.
(36) Habtemariam, A.; Betanzos-Lara, S.; Sadler, P. J. Di-μ-chloro(ethylbenzoate)diruthenium(II), $[(\eta^6\text{-etb})RuCl_2]_2$. In *Inorganic Synthesis*, Rauchfuss, T. B., Ed. John Wiley & Sons: 2010; p 148.
(37) González-Fernández, R.; Crochet, P.; Cadierno, V. Half-sandwich ruthenium(II) complexes with tethered arene-phosphinite ligands: synthesis, structure and application in catalytic cross dehydrogenative coupling reactions of silanes and alcohols. *Dalton Trans.* **2020**, *49*, 210−222.
(38) Martínez-Peña, F.; Pizarro, A. M. Control of reversible activation dynamics of $[Ru\{\eta^6{:}\kappa^1\text{-}C_6H_5(C_6H_4)NH_2\}(XY)]^{n+}$ and the effect of chelating-ligand variation. *Chem. − Eur. J.* **2017**, *23*, 16231−16241.
(39) Çetinkaya, B.; Demir, S.; Özdemir, I.; Toupet, L.; Séméril, D.; Bruneau, C.; Dixneuf, P. H. η^6-mesityl,η^1-imidazolinylidene-carbene-ruthenium(II) complexes: catalytic activity of their allenylidene derivatives in alkene metathesis and cycloisomerisation reactions. *Chem. − Eur. J.* **2003**, *9*, 2323−2330.
(40) Wübbolt, S.; Maji, M. S.; Irran, E.; Oestreich, M. A tethered Ru-S complex with an axial chiral thiolate ligand for cooperative Si-H bond activation: Application to enantioselective imine reduction. *Chem. − Eur. J.* **2017**, *23*, 6213−6219.
(41) Aznar, R.; Grabulosa, A.; Mannu, A.; Muller, G.; Sainz, D.; Moreno, V.; Font-Bardia, M.; Calvet, T.; Lorenzo, J. $[RuCl_2(\eta^6\text{-}p\text{-cymene})(P^*)]$ and $[RuCl_2(\kappa\text{-}P^*\text{-}\eta^6\text{-arene})]$ complexes containing P-stereogenic hosphines. Activity in transfer hydrogenation and interactions with DNA. *Organometallics* **2013**, *32*, 2344−2362.
(42) Stodt, R.; Gencaslan, S.; Müller, I. M.; Sheldrick, W. S. Preparation, Reactivity and Peptide Labelling Properties of (η^6-Arene)ruthenium(II) Complexes with Pendant Carboxylate Groups. *Eur. J. Inorg. Chem.* **2003**, *10*, 1873−1882.
(43) Tönnemann, J.; Risse, J.; Grote, Z.; Scopelliti, R.; Severin, K. Efficient and rapid synthesis of chlorido-bridged half-sandwich complexes of ruthenium, rhodium, and iridium by microwave heating. *Eur. J. Inorg. Chem.* **2013**, *2013*, 4558−4562.
(44) Ang, W. H.; Daldini, E.; Juillerat-Jeanneret, L.; Dyson, P. J. Strategy To Tether Organometallic Ruthenium−Arene Anticancer Compounds to Recombinant Human Serum Albumin. *Inorg. Chem.* **2007**, *46*, 9048−9050.
(45) Ang, W. H.; Parker, L. J.; De Luca, A.; Juillerat-Jeanneret, L.; Morton, C. J.; Lo Bello, M.; Parker, M. W.; Dyson, P. J. Rational Design of an Organometallic Glutathione Transferase Inhibitor. *Angew. Chem., Int. Ed.* **2009**, *48*, 3854−3857.
(46) Kilpin, K. J.; Clavel, C. M.; Edafe, F.; Dyson, P. J. Naphthalimide-Tagged Ruthenium−Arene Anticancer Complexes: Combining Coordination with Intercalation. *Organometallics* **2012**, *31*, 7031−7039.
(47) Nazarov, A. A.; Risse, J.; Ang, W. H.; Schmitt, F.; Zava, O.; Ruggi, A.; Groessl, M.; Scopelitti, R.; Juillerat-Jeanneret, L.; Hartinger, C. G.; Dyson, P. J. Anthracene-Tethered Ruthenium(II) Arene Complexes as Tools To Visualize the Cellular Localization of Putative Organometallic Anticancer Compounds. *Inorg. Chem.* **2012**, *51*, 3633−3639.
(48) Reiner, T.; Waibel, M.; Marziale, A. N.; Jantke, D.; Kiefer, F. J.; Fässler, T. F.; Eppinger, J. η^6-Arene complexes of ruthenium and osmium with pendant donor functionalities. *J. Organomet. Chem.* **2010**, *695*, 2667−2672.
(49) Wilson, C. S.; Prior, T. J.; Sandland, J.; Savoie, H.; Boyle, R. W.; Murray, B. S. Homo- and hetero-dinuclear arene-linked osmium(II) and ruthenium(II) organometallics: Probing the impact of metal variation on reactivity and biological activity. *Chem. − Eur. J.* **2020**, *26*, 11593−11603.
(50) Zhou, X.; He, X.; Lin, J.; Zhuo, Q.; Chen, Z.; Zhang, H.; Wang, J.; Xia, H. Reactions of Osmium Hydrido Alkenylcarbyne with Allenoates: Insertion and [3 + 2] Annulation. *Organometallics* **2015**, *34*, 1742−1750.
(51) Soldevila-Barreda, J. J.; Fawibe, K. B.; Azmanova, M.; Rafols, L.; Pitto-Barry, A.; Eke, U. B.; Barry, N. P. E. Synthesis, Characterisation and In Vitro Anticancer Activity of Catalytically Active Indole-Based Half-Sandwich Complexes. *Molecules* **2020**, *25*, 4540.
(52) Alessio, E. Synthesis and Reactivity of Ru-, Os-, Rh-, and Ir-Halide−Sulfoxide Complexes. *Chem. Rev.* **2004**, *104*, 4203−4242.
(53) Battistin, F.; Balducci, G.; Milani, B.; Alessio, E. Water-Soluble Ruthenium(II) Carbonyls with 1,3,5-Triaza-7-phosphoadamantane. *Inorg. Chem.* **2018**, *57*, 6991−7005.
(54) Alessio, E.; Serli, B.; Zangrando, E.; Calligaris, M.; Panina, N. S. Geometrical and Linkage Isomers of $[OsCl_2(dmso)_4]$− The Complete Picture. *Eur. J. Inorg. Chem.* **2003**, *2003*, 3160−3166.
(55) Needham, R. J.; Habtemariam, A.; Barry, N. P. E.; Clarkson, G.; Sadler, P. J. Halide Control of N,N-Coordination versus N,C-Cyclometalation and Stereospecific Phenyl Ring Deuteration of Osmium(II) p-Cymene Phenylazobenzothiazole Complexes. *Organometallics* **2017**, *36*, 4367−4375.
(56) Martínez-Peña, F.; Infante-Tadeo, S.; Habtemariam, A.; Pizarro, A. M. Reversible pH-responsive behavior of ruthenium(II) arene complexes with tethered carboxylate. *Inorg. Chem.* **2018**, *57*, 5657−5668.
(57) Zhong, L.; Arnér, E. S.; Holmgren, A. Structure and mechanism of mammalian thioredoxin reductase: the active site is a redox-active selenolthiol/selenenylsulfide formed from the conserved cysteine-selenocysteine sequence. *Proc. Natl. Acad. Sci. U. S. A.* **2000**, *97*, 5854−5859.
(58) Krężel, A.; Bal, W. A formula for correlating pK_a values determined in D_2O and H_2O. *J. Inorg. Biochem.* **2004**, *98*, 161−166.

https://doi.org/10.1021/acs.inorgchem.2c03246
Inorg. Chem. 2022, 61, 18970−18978